IOSR Journal of Electrical and Electronics Engineering (IOSR-JEEE)
e-ISSN: 2278-1676, p-ISSN: 2320-3331, Volume 16, Issue 6 Ser. I (Nov. – Dec. 2021), PP 09-15
www.iosrjournals.org

Air Conduit Disinfectors Using Ultraviolet C-band Light-Emitting Diodes

Jianping Zhang[1*], Ling Zhou[1], Ying Gao[1], Maria Topete[1], Alexander Lunev[1], Frank Harder[1], Michael Krames[2]
[1]*Bolb Inc., 52 Wright Brothers Avenue, Livermore, California, 94551, USA*
[2]*Arkesso LLC., 2625 Middlefield Road, Palo Alto, California 94306, USA*

Abstract
Airborne transmission of respiratory viruses can cause pandemics. To understand the effectiveness of using ultraviolet (UV) C-band light for indoor air disinfection, we analyze UV light dose delivery to air and other fluids in conduit disinfectors. Analytical dose equations are derived respectively for a circular non-reflective conduit enclosing a linear UV light source and a square reflective conduit with a directional UV light source. It is found that the fluid UV absorption coefficient α plays an important role in determining the UV light distribution for efficient dose delivery. For opaque fluids of α larger than 0.03 cm^{-1}, distributed instead of concentrated UV light can deliver dose more efficiently. Meanwhile, for transparent fluids with α less than 0.03 cm^{-1}, a directional UV light source can be far more efficient in dose delivery to flowing fluids than a linear UV light source. We then show that the state-of-the-art UV C-band (UVC) LEDs of wall-plug-efficiency (WPE) 6-10% delivering a light cone with a full width at half maximum (FWHM) angle of 9.5^o can outperform linear mercury lamps of WPE 30% for flowing air disinfection, taking advantage of the light beam collimation capability of the UVC LEDs. Our model further shows that these highly collimated UVC LED beams of optical power 2.5W can treat air flow 100,000 liters per minute to eliminate severe acute respiratory syndrome coronavirus 2 (SARS-CoV-2).

Keywords: *Air disinfection, COVID-19, ultraviolet light, UVC LEDs, SARS-CoV-2.*

Date of Submission: 20-11-2021 Date of Acceptance: 04-12-2021

I. Introduction

Two years into the ongoing coronavirus disease 2019 (COVID-19) pandemic, global evidence reveals that airborne COVID-19 virions are mainly responsible for the pandemic's rapid world-wide spread ([1]). Effective and affordable indoor air disinfection technologies are thus highly desirable for mitigation of COVID-19 and prevention of possible future pandemics. Various research groups have measured the ultraviolet C-band (UVC) light dose for 99.9% deactivation rate of COVID-19 viruses (i.e., severe acute respiratory syndrome coronavirus 2, or SARS-CoV-2) to be within 1.8-3.7 mJ/cm^2 ([2], [3]). This appoints UVC light as a very promising means for stoppage of COVID-19 virus transmission.

Meanwhile, solid-state UVC light sources such as UVC light-emitting diodes (LEDs) have been developed for the last 20 years ([4]-[13]), and the state-of-the-art UVC LEDs can operate with wall-plug-efficiency (WPE) 8.5%-9.5% at peak emission wavelengths of 265-280 nm, thanks to a UVC-transparent epitaxial structure ([14], [15]). Even though large headroom for performance improvement still exists for UVC LEDs to catch up with the conventional UVC mercury lamp's WPE of 15-40% ([16]), a fair question deserving a solid answer is what disinfection applications are ready now for the state-of-the-art UVC LEDs. Specifically, it would be timely for the field of interest to understand the potential and possibility of UVC LEDs in disinfecting flowing fluids such as air and drinking water, which are two main media for widespread disease propagation.

For this purpose and for better understanding of UVC light dose delivery physics, in the following content we set out to obtain analytical dose equations, by analyzing UVC light dose delivery to flowing fluids in two simplified yet highly practical fluid disinfection chambers, a circular and a square conduit. Analytical dose equations are derived for a circular non-reflective conduit enclosing a linear light source (such as a germicidal mercury lamp) and a square reflective conduit with a directional light source (made by of UVC LED arrays), respectively. It is found that the fluid UV absorption coefficient α plays an important role in determining the optimum UV light distribution for efficient dose delivery. For opaque fluids of α larger than 0.03 cm^{-1}, distributed instead of concentrated UV light delivers dose better. For transparent fluids of α less than 0.03 cm^{-1}, directional UV light sources are more efficient in dose delivery to flowing fluid than linear UV light sources. The more parallel the light beam is to the flowing fluid, the more efficient the dose delivery performs. Mostly strikingly, our model shows that being able to collimate beams the state-of-the-art UVC LEDs of WPE 6-10% can result in more efficient dose delivery hence better disinfection efficacy as compared to the linear mercury germicidal lamps of WPE 30% in flowing air disinfection. In particular, we show that for a square conduit disinfector of cross-section 12”×12” with inner surface effective reflectance 90%, a coaxially installed highly collimated UVC LED light source of optical power 2.5W can deliver SARS-CoV-2 elimination dose 3.7 mJ/cm^2 to flowing air with flow rate up to 100,000 liters per minute.

II. Fluid Disinfector Models

As illustrated in Fig. 1, consider a circular non-reflective conduit disinfector for flowing fluid, with diameter $D=2R_0$ and length L. Sitting on the axis of the conduit is a linear UVC light source (e.g., a germicidal mercury lamp) of equal length L and diameter $2r_0$, emitting optical power P uniformly and axially. A fluid to be disinfected is flowing through the conduit from left to right with flow rate G and UVC light absorption coefficient α. For simplicity, the fluid under consideration is of laminar flow and has small viscosity so that interfacial boundary layer is negligible.

As such, a fluid layer of a cylindrical surface r ($r_0 \le r \le R_0$) receives UVC dose $J(r)$: $J(r) = \frac{Pe^{-\alpha(r-r_0)}}{2\pi rL}\frac{L}{\frac{G}{\pi(R_0^2-r_0^2)}} = e^{\alpha r_0}\frac{P(R_0^2-r_0^2)}{2G}\frac{e^{-\alpha r}}{r}$. And the total flowing fluid receives average dose: $\bar{J} = \frac{1}{R_0-r_0}\int_{r_0}^{R_0} J(r)dr = e^{\alpha r_0}\frac{P(R_0+r_0)}{2G}\int_{r_0}^{R_0}\frac{e^{-\alpha r}}{r}dr$, which can be expanded and calculated via eq. (1):

$$\bar{J} = e^{\alpha r_0}\frac{P(R_0+r_0)}{2G}\left[ln\frac{R_0}{r_0} + \sum_{n=1}^{\infty}\frac{(-\alpha)^n(R_0^n-r_0^n)}{n.n!}\right] \quad (1)$$

For fluid such as air, if absorption coefficient α or αR_0 approaches zero, then the average dose is given by:

$$\bar{J} = \frac{P(R_0+r_0)}{2G}ln\frac{R_0}{r_0} \quad (2)$$

In this case if the conduit disinfector is of effective UVC reflectance R then the dose would be expected to be enhanced by a factor $\frac{1}{1-R}$.

Illustrated in Fig. 2 is a square conduit for flowing fluid disinfection, with cross-section dimensions $L_y = L_z = D$, and effective UVC reflectance R. A UVC LED array light panel of size D^2 is placed at one end of the conduit for emitting directional light beam of optical power $P_0(\theta)$ along the axis of the conduit, where θ is the light impinge angle, i.e., the angle between the light beam and the axis of the conduit. The fluid under consideration is of laminar flow and has small viscosity so that interfacial boundary layer is negligible. These assumptions are taken to facilitate an analytical dose equation to understand the dose delivery process in fluid conduit disinfectors.

Consider the dose delivery process between n-th and $(n+1)$-th reflections. After n-th reflection, the impinge power becomes $P_n = P_0R^ne^{-\alpha nD\csc\theta}$. P_n has a vertical component $P_n\,sin\,\theta$ and a horizontal component $P_n\cos\theta$ impinging perpendicular and parallel to fluid flow G within the square conduit, respectively. The horizontal component power $P_n\cos\theta$ impinges perpendicularly on a cross-section area of L_zL_y, and the vertical component $P_n\,sin\,\theta$ impinges perpendicularly on an area of $L_zL_y cot\,\theta$. Between n-th and $(n+1)$-th reflections, the fluid flow’s exposure time to UVC light is $t_n = \frac{L_z^2L_y\cot\theta}{G}$, hence the horizontal and vertical power components deliver doses $J_{n1} = \frac{P_n\cos\theta}{\alpha G}(1-e^{-\alpha D\cot\theta})$ and $J_{n2} = \frac{P_n\sin\theta}{\alpha G}(1-e^{-\alpha D})$ to fluid flow between n-th and $(n+1)$-th reflections, respectively. Summing up J_{n1} and J_{n2} for all reflections leads to the following equation for average dose to the fluid:

$$J = \frac{P_0}{\alpha G}\left(\cos\theta - \cos\theta e^{-\alpha D\cot\theta} + \sin\theta - \sin\theta\, e^{-\alpha D}\right)\frac{1-R^{n+1}e^{-\alpha(n+1)D\csc\theta}}{1-Re^{-\alpha D\csc\theta}} \quad (3)$$

When $n \to \infty, and\,\theta > 0$, i.e., for unlimited reflections, eq. (3) becomes,

$$J = \frac{P_0}{\alpha G}\left(\cos\theta - \cos\theta e^{-\alpha D\cot\theta} + \sin\theta - \sin\theta\, e^{-\alpha D}\right)\frac{1}{1-Re^{-\alpha D\csc\theta}} \quad (4)$$

When $n \to \infty, and\,\theta \to 0$, if the conduit is of finite length L, $D\csc\theta$ and $D\cot\theta$ will be replaced by L, so,

$$J = \frac{P_0}{\alpha G}\frac{1-e^{-\alpha L}}{1-Re^{-\alpha L}} \quad (5)$$

Notice here that if R=0, eq. (5) becomes,

$$J = \frac{P_0}{\alpha G}(1-e^{-\alpha L}) \quad (6)$$

If α is small, for example, for air $\alpha \in [10^{-6}, 10^{-4}]$ cm^{-1}, eq. (6) becomes,

$$J = \frac{P_0L}{G} \quad (7)$$

Also, if $L \gg \frac{1}{\alpha}$, eq. (6) becomes,

$$J = \frac{P_0}{\alpha G} \quad (8)$$

When the light panel emits light of a certain power angular distribution, then the total dose delivered into the flowing fluid is the integral of eq. (4) over $-\frac{\pi}{2} \le \theta \le -\frac{\pi}{2}$, i.e.,

$$J = \int_{-\frac{\pi}{2}}^{\frac{\pi}{2}} d\theta \frac{P_0(\theta)}{\alpha G} (\cos\theta + \sin\theta - \cos\theta e^{-\alpha D \cot\theta} - \sin\theta\, e^{-\alpha D}) \frac{1}{1 - Re^{-\alpha D \csc\theta}} \quad (9)$$

III. Results And Discussion

3.1 Perfectly collimated light source and linear light source in air disinfection

Air as a fluid has very small UVC absorption coefficient. Here we can quickly compare the dose delivered for air disinfection using two kinds of non-reflective conduit disinfectors: one with a linear light source where the dose is given by eq. (2), one with a perfectly collimated ($\theta = 0$) UVC LED light source where dose is given by eq. (7). For the same optical power, the ratio (ρ) of the dose delivered by the UVC LED collimated beam conduit disinfector to that delivered by the linear UVC light source conduit disinfector is,

$$\rho = \frac{2L}{(R_0 + r_0) \ln \frac{R_0}{r_0}} \quad (10)$$

As seen, ρ only depends on the conduit geometrical dimensions. For a conduit, its length can always be designed to be much larger than its diameter or lateral dimension, meaning that ρ can be much larger than 1. This means that conduit disinfectors equipped with collimated UVC light sources are in general more effective for air disinfection, as compared to the ones with linear UVC light sources.

3.2 The effect of UVC light absorption coefficient on dose delivered to fluids

With the above two conduit disinfector models set up, we can use some practical design parameters to compare the dose delivery for the conduit disinfectors illustrated in Figs. 1 and 2. Firstly, consider fluid disinfection in the square conduit disinfector shown in Fig. 2. We apply eq. (4) and plot doses as function of light impinging angle θ for fluids of different UVC absorption coefficient α's, using parameters D=12", R=0.9, G=1000 liters per minute (lpm) and P_0=2.5 W. The results are presented in Fig. 3. As seen, when α is small, e.g., $\alpha \le 10^{-3}$ cm^{-1}, dose delivery is more effective at small impinge angles; for large α's, e.g., $\alpha \ge 10^{-2}$ cm^{-1}, dose delivery is not very sensitive to impinge angles. This suggests that for fluids of small α's, such as air ($\alpha \in [10^{-6}, 10^{-4}]$ cm^{-1}) and drinking water ($\alpha \in [2\times10^{-4}, 10^{-2}]$ cm^{-1}), using small light impinging angles can result in more efficient UVC dose delivery. For a sufficient long conduit ($L \gg \frac{1}{\alpha}$), using zero impinge angle (i.e., a collimated light source) can achieve the largest dose, which approaches $J = \frac{P_0}{\alpha G}$. For air disinfection, zero or small impinging angle UVC light can deliver significant dose as air has very small UVC absorption coefficient, meaning that a small collimated UVC light power can disinfect a large air flow.

3.3 Comparison of linear and directional UVC light sources for air and fluid disinfection

Compared to the linear mercury UVC lamps, UVC LEDs with their small etendue have an advantage of producing a collimated beam within a small geometry, as UVC LED's far field intensity pattern can be modified via a small secondary optics such as a reflector or lens. Fig. 4 plots a far field intensity pattern $I(r,\theta,\phi)$for a commercially available narrow-beam UVC LED (Bolb Inc., Livermore CA, USA.) measured at radius r=1 meter. This LED is equipped with a narrow beam rotationally symmetrical reflector, as a result, the far field intensity $I(r,\theta,\phi)$ has no azimuth angle (ϕ) dependence, i.e., $I(r,\theta,\phi)=I(r,\theta)$. As shown, the full width at half maximum (FWHM) angle is 9.5^{o}. In order to be able to use eq. (9) to calculate dose for the conduit disinfector illustrated in Fig. 2, we need to know the LED's optical power angular distribution, which can be converted from the far field intensity pattern via $dP = P(\theta)d\theta = I(r,\theta)2\pi r^2 sin\theta d\theta$ (at r=1 meter). Upon conversion, it is found that 43% and 67% of the total optical power of this LED are within light cones of cone angles (2θ) of 20^{o} and 40^{o}, respectively, indicating this LED being a directional and highly concentrated light source. For the following calculations, multiple such narrow-beam LEDs are assumed to form the light panel for the conduit disinfector illustrated in Fig. 2.

We then investigate the effect of fluid UVC absorption coefficient on dose delivery for the two types of disinfectors, i.e., the Hg lamp and UVC LED conduit disinfectors illustrated in Figs. 1 and 2, respectively. The UVC optical power are fixed to be 2.5 W, assumed to be delivered by the linear Hg lamp and directional UVC LED light panel (this is a reasonable output power obtainable with commercially available UVC LED arrays) for their respective conduit disinfectors. The parameters for the Hg lamp conduit are: R=0 (non-reflective), $2R_0$ =30 cm, $2r_0$ =5 cm, L=120 cm. The parameters for the UVC LED conduit are: D =30 cm, L = 120 cm, with various effective UVC reflectance R's including R=0. Shown in Fig. 5 are the calculated UVC doses (via eqs. (1)

and (9)) for 500 lpm flowing fluids of varying absorption coefficients in the two conduit disinfectors. As seen, for effective UVC reflectance R=0 and absorption coefficient $\alpha \leq 10^{-3}$ cm^{-1}, the UVC LED conduit disinfector delivers about 6 times of the dose that the Hg lamp conduit disinfector can, suggesting that the UVC LED conduit disinfector is far more efficient in dose delivery for transparent fluids such as air and drinking water. This is because that the collimated UVC light can have more probability to interact with air and reduce energy loss due to reflections. With the same UVC optical power and similar disinfection conduit geometry the narrow-beam UVC LEDs delivering 6 times dose as compared to the linear Hg lamp implies that even though presently the UVC LEDs are of less WPE (6-10%, as compared to Hg lamps' WPE 15-30%), with the right disinfector design UVC LEDs today can readily match and even outperform Hg lamps in air disinfection. Also notice that for transparent fluids ($\alpha \leq 10^{-3}$ cm^{-1}) a UVC LED conduit disinfector of effective reflectance R can further enhance dose delivery by a factor of $\sim\frac{1}{1-R}$, as compared to one with zero reflectance. For opaque fluids ($\alpha \geq 3 \times 10^{-2}$ cm^{-1}) such as milk, juice and greywater, Hg lamp conduit disinfector starts to win in terms of dose delivery in this example. This suggests for highly absorptive fluids, increasing illumination area with distributed UVC light can do better in dose delivery. This is understandable as opaque fluids absorb UVC light strongly and prevent UVC light penetration.

We now focus on clean air disinfection using the abovementioned conduit disinfectors. Fig. 6 presents the calculated UVC doses to air in the flow rate range of 10^3 to 10^5 lpm for three conduit disinfectors, assuming $\alpha = 10^{-6}$ cm^{-1}.The conduit disinfectors are of lateral dimension D=30.5 cm, L=120 cm, and UVC optical power 2.5 W. Again, when R=0 the UVC LED conduit disinfector delivers about 6 times of the dose that the Hg lamp conduit disinfector can for the same air flow. From eq. (10), one would get $\rho = 7.65$ from the conduit dimensions we used above if the UVC light intensity FWHM angleof the UVC LED light panel is zero instead of 9.5^{o}.Also, the UVC LED conduit disinfector can further enhance dose delivery to air flow by a factor of $\frac{1}{1-R}$ if it has an effective UVC reflectance R. The factor $\frac{1}{1-R}$ is significant as R approaches 1. For example, deposited aluminum films and micro-porous Teflon layers can have UVC reflectance of 0.9 and 0.99, respectively. As a result, notably the UVC LED conduit disinfector of D=30.5 cm, L=120 cm, P=2.5 W and R=0.9 can deliver SARS-CoV-2 elimination UVC dose 3.7 mJ/cm^2 to air with flow rate of 10^5 lpm, which is the designed air flow rate for the central air conditioner system of a 3500 square feet family house in the United States.

IV. Conclusions

In summary, linear and directional light source conduit disinfectors are studied in terms of UVC dose delivery to flowing fluids, and the respective analytical dose equations are derived. We find that the fluid UV absorption coefficient α plays an important role in determining the UV light distribution for efficient dose delivery. For transparent fluids with α less than 0.03 cm^{-1}, directional UV light source can be far more efficient in dose delivery to flowing fluid than linear UV light source. For opaque fluids of α larger than 0.03 cm^{-1}, it is better to use distributed instead of concentrated UV light to deliver dose. Taking the advantage of light beam collimation of UVC LEDs, the state-of-the-art UVC LEDs of WPE 6-10% can outperform mercury lamps of WPE 30% in flowing air and drinking water disinfections. Our model shows that highly collimated UVC LED beam of optical power 2.5W can treat air flow 100,000 lpm to eliminate SARS-CoV-2 in air-handling systems used in standard households.

DISCLAIMER

All Bolb authors and contributors were full time employees of Bolb Inc during their respective contributions to this effort. No financial compensation was received outside of the contributors' regular monetary compensation due to their employment at Bolb Inc.

References

[1]. Zhang R., Li Y., Zhang A., Wang Y., and Molina M. Identifying airborne transmission as the dominant route for the spread of COVID-19. Proc. Natl. Acad. Sci. U.S.A. **117**, 14857-14863 (2020). https://doi.org/10.1073/pnas.2009637117

[2]. Minamikawa T., Koma T., Suzuki A., Mizuno T., Nagamatsu K., Arimochi H., Tsuchiya K., Matsuoka K., Yasui T., Yasutomo K., and Nomaguchi M. Quantitative evaluation of SARS‐CoV‐2 inactivation using a deep ultraviolet light‐emitting diode. Scientific Reports **11**, 5070 (2021). https://doi.org/10.1038/s41598-021-84592-0

[3]. Biasin M., Bianco A., Pareschi G., Cavalleri A., Cavatorta C., Fenizia C., Galli P., Lessio L., Lualdi M., Tombetti E., Ambrosi A., Redaelli E., Saulle I., Trabattoni D., Zanutta A., and Clerici M. UV‐C irradiation is highly effective in inactivating SARS‐CoV‐2 replication. Scientific Reports **11**, 6260 (2021). https://doi.org/10.1038/s41598-021-85425-w

[4]. Zhang J. P., Chitnis A., Adivarahan V., Wu S., Mandavilli V., Pachipulusu R., Shatalov M., Simin G., Yang J. W., and Khan A. Milliwatt power deep ultraviolet light-emitting diodes over sapphire with emission at 278 nm. Appl. Phys. Lett. **81**, 4910 (2002). https://doi.org/10.1063/1.1531835

[5]. Zhang J. P., Hu X., Bilenko Y., Deng J., Lunev A., Shur M. S., Gaska R., Shatalov M., Yang J., and Khan M. A. AlGaN-based 280nm light-emitting diodes with continuous-wave power exceeding 1mW at 25mA. Appl. Phys. Lett. **85**, 5532 (2004). https://doi.org/10.1063/1.1831557

[6]. Khan A., Balakrishnan K., and Katona T. Ultraviolet light-emitting diodes based on group three nitrides. Nature Photonics **2**, 77-84 (2008). https://doi.org/10.1038/nphoton.2007.293

[7]. Hirayama H, Yatabe T, Noguchi N, Ohashi T, Kamata N. 231–261 nm AlGaN deep ultraviolet light-emitting diodes fabricated on AlN multilayer buffers grown by ammonia pulse-flow method on sapphire. Appl. Phys. Lett. **91**, 071901 (2007). https://doi.org/10.1063/1.2770662

[8]. Fujioka A, Misaki T, Murayama T, Narukawa Y, Mukai T. Improvement in output power of 280-nm deep ultraviolet light-emitting diode by using AlGaN multi quantum wells. Applied Physics Express **3**, 041001 (2010). https://iopscience.iop.org/article/10.1143/APEX.3.041001

[9]. Shatalov M., Sun W., Lunev A., Hu X., Dobrinsky A., Bilenko Y., Yang J., Shur M., Gaska R., Moe C., Garrett G., and Wraback M. AlGaN Deep-Ultraviolet Light-Emitting Diodes with External Quantum Efficiency above 10%. Applied Physics Express **5**,082101 (2012). https://iopscience.iop.org/article/10.1143/APEX.5.082101

[10]. Kneissl M. III-nitride ultraviolet emitters. In: Springer Series in Material Science 227.Woodhead Publishing, ISSN 0933-033X, (2016).

[11]. Inoue S, Tamari N, Taniguchi M. 150 mW deep-ultraviolet light-emitting diodes with large-area AlN nano-photonic light extraction structure emitting at 265 nm. Appl. Phys. Lett. **11**0,141106 (2017). https://doi.org/10.1063/1.4978855

[12]. Takano T., Mino T., Sakai J., Noguchi N., Tsubaki K., and Hirayama H. Deep-ultraviolet light-emitting diodes with external quantum efficiency higher than 20% at 275 nm achieved by improving light-extraction efficiency. Applied Physics Express **10**, 031002 (2017). https://iopscience.iop.org/article/10.7567/APEX.10.031002/meta

[13]. Kneissl M., Seong T., Han J., and Amano H. The emergence and prospects of deep-ultraviolet light-emitting diode technologies. Nature Photonics **13**, 233-244 (2019). https://doi.org/10.1038/s41566-019-0359-9

[14]. Zhang J. P., Gao Y., Zhou L., Gil Y., Kim K. Surface hole gas enabled transparent deep ultraviolet light-emitting diode. Semicon. Sci. Technol. **33**, 07LT01 (2018). https://doi.org/10.1088/1361-6641/aac7c1

[15]. Zhang J. P., Gao Y., Zhou L., Gil Y., Kim K. Transparent deep ultraviolet light-emitting diodes with a p-type AlN ohmic contact layer. Proc. Of SPIE **10940**, 1094002 (2019). https://doi.org/10.1117/12.2506918

[16]. Zhang H., Han Q., and Zhang S. 254 nm Radiant Efficiency of High Output Low Pressure Mercury Discharge Lamps with Neon-Argon Buffer Gas. Applied Mechanics and Materials **325-326**, 409-412 (2013). https://doi.org/10.4028/www.scientific.net/AMM.325-326.409

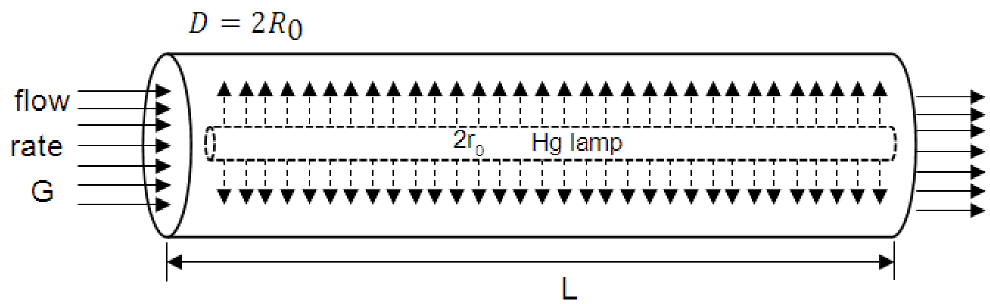

Fig. 1, Illustration of a circular conduit disinfector for flowing fluid, with a linear UVC light source sitting on the conduit axis.

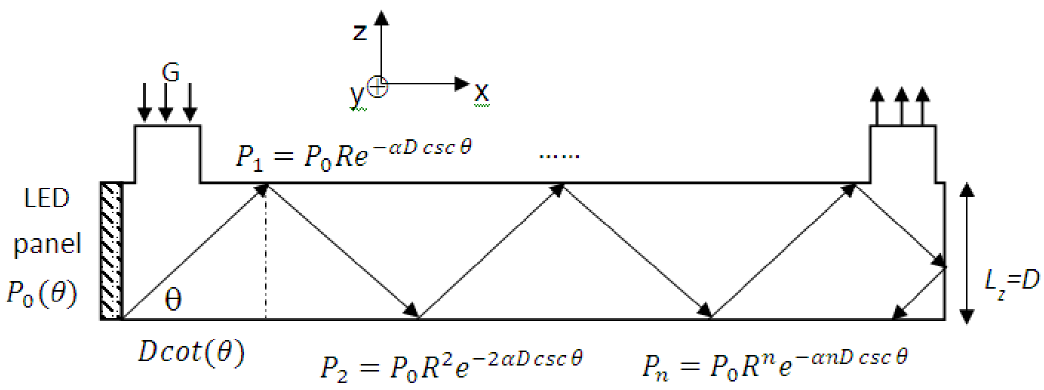

Fig. 2, Illustration of a square conduit disinfector for flowing fluid, with a directional UVC light panel sitting at one end of the conduit.

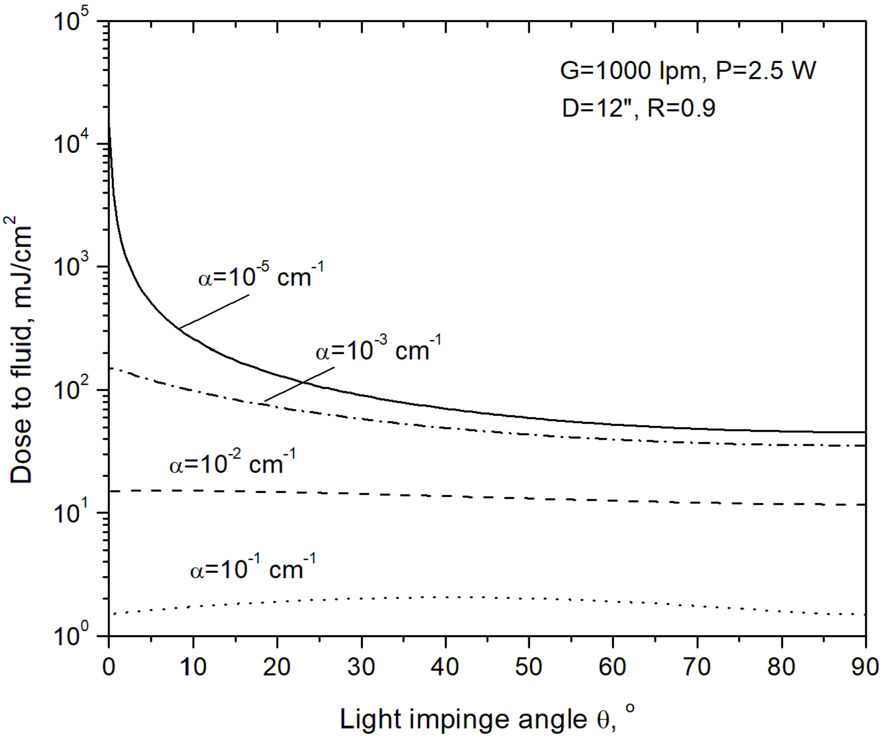

Fig. 3, Calculated UVC doses as function of light impinge angles for flowing fluids of different UVC absorption coefficients for a conduit disinfector illustrated in Fig. 2.

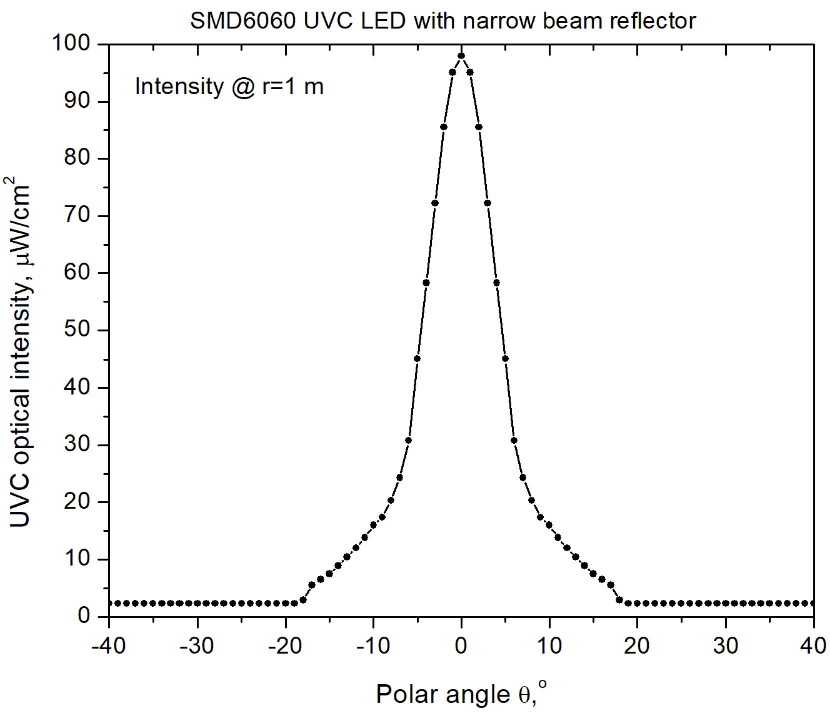

Fig. 4, Optical intensity angular distribution of a narrow beam SMD6060 UVC LED measured at radius 1 meter.

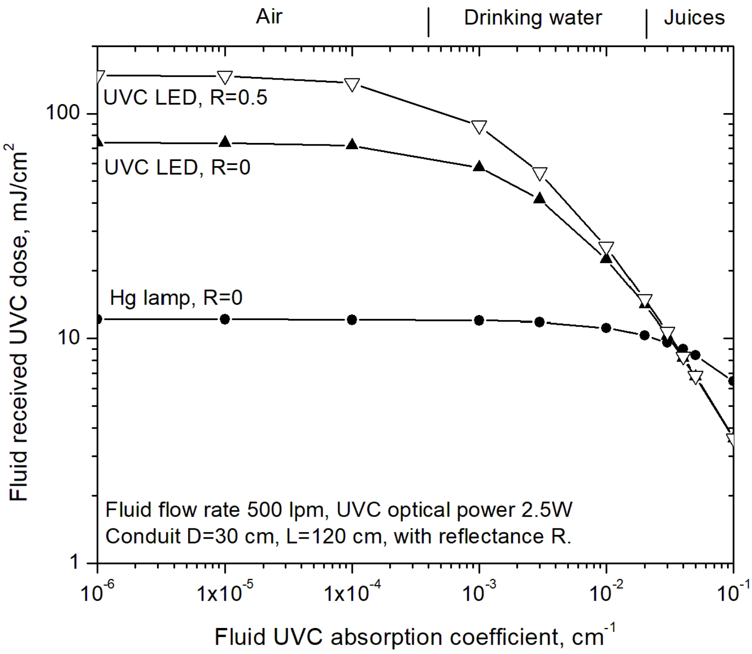

Fig. 5, Calculated UVC doses for 500 lpm flowing fluids of varying absorption coefficients in different conduit disinfectors.

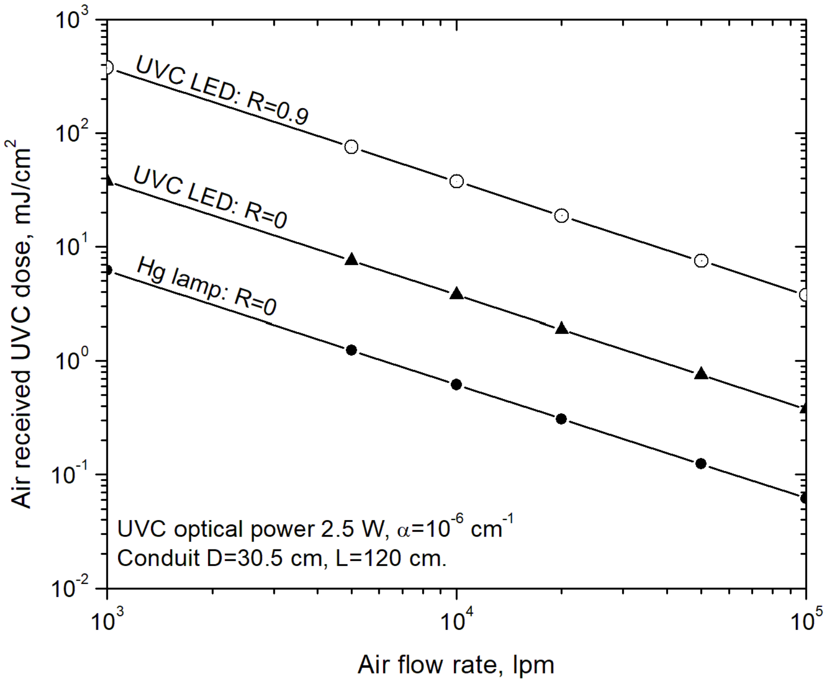

Fig. 6, Calculated UVC doses to air as function of air flow rate for different conduit disinfectors.

Jianping Zhang, et. al. "Air Conduit Disinfectors Using Ultraviolet C-band Light-Emitting Diodes." *IOSR Journal of Electrical and Electronics Engineering (IOSR-JEEE)*, 16(6), (2021): pp. 09-15.